Targeting Primary Human Ph$^+$ B-Cell Precursor Leukemia-Engrafted SCID Mice Using Radiolabeled Anti-CD19 Monoclonal Antibodies

Paul Mitchell, MBBS[1]; Fook-Thean Lee, PhD[2]; Cathrine Hall, BSc[2]; Angela Rigopoulos, MSc[2]; Fiona E. Smyth, BSc[2]; Anne-Marie Hekman, PhD[3]; Gijs M. van Schijndel, PhD[4]; Ray Powles, PhD[5]; Martin W. Brechbiel, PhD[6]; and Andrew M. Scott, MD[2,7]

[1]Ludwig Medical Oncology Unit, Ludwig Institute For Cancer Research, Melbourne Tumour Biology Branch, Austin and Repatriation Medical Centre, Melbourne, Victoria, Australia; [2]Tumour Targeting Program, Ludwig Institute For Cancer Research, Melbourne Tumour Biology Branch, Austin and Repatriation Medical Centre, Melbourne, Victoria, Australia; [3]Department of Immunology, The Netherlands Cancer Institute, Amsterdam, The Netherlands; [4]Sanquin Research and Landsteiner Laboratory, University of Amsterdam, Amsterdam, The Netherlands; [5]Leukemia Unit, Royal Marsden Hospital, Surrey, United Kingdom; [6]Radioimmune and Inorganic Chemistry Section, National Cancer Institute, National Institutes of Health, Bethesda, Maryland; and [7]Department of Nuclear Medicine and Centre for PET, Austin and Repatriation Medical Centre, Melbourne, Victoria, Australia

The Philadelphia chromosome translocation (Ph$^+$) confers a poor prognosis in patients with acute lymphocytic leukemia (ALL). CD19 is highly expressed (CD19$^+$) on ALL cells and is an attractive target for antibody-based therapies. CLB-CD19 is an IgG1κ murine monoclonal antibody (mAb) directed against an epitope on the CD19 antigen. **Methods:** Radiolabeled CLB-CD19 antibody was evaluated for targeting ALL in a severe combined immunodeficient (SCID) mouse model engrafted with primary human leukemia cells. Lodgment of CD19$^+$ ALL cells in spleen and liver was confirmed using immunohistochemistry analyses. Circulating CD19$^+$ ALL cells in blood were also detected by flow cytometry. **Results:** Antibody was labeled directly with the radiohalogen ^{125}I and radiometal ^{111}In via the bifunctional metal ion chelate CHX-A″-diethylenetriaminepentaacetic acid (DTPA) with retention of immunoreactivities. After intravenous injection of radioconjugates, biodistribution studies showed rapid localization of the ^{111}In-conjugate to leukemia-infiltrated spleen, reaching a maximum (mean ± SD) of 72.78 ± 13.67 % injected dose per gram of tissue (%ID/g) by 24 h after injection. In contrast, peak localization of coinjected ^{125}I-CLB-CD19 occurred by 4 h and was significantly lower (11.41 ± 12.79 %ID/g) ($P < 0.001$). Uptake of ^{111}In-conjugate in the liver containing tumor was also evident but not in other normal tissues. Uptake of radiolabeled CLB-CD19 in tumor-bearing organs was specific, as uptake of radiolabeled isotype-matched antibody control was low. Gamma-camera imaging detected the uptake of ^{111}In-CHX-A″-DTPA CLB-CD19 in enlarged tumor-bearing spleen of engrafted mice. A single injection of 32 μg CLB-CD19 mAb had a delayed suppressive effect on the level of circulatory leukemia cells in surviving mice and extended the median survival from 48.5 to 58 d ($n = 8$; $P = 0.03$). **Conclusion:** The radiolabeled anti-CD19 antibody showed specific targeting and rapid internalization in ALL cell–engrafted SCID mice and may also be used for selective intracellular delivery of cytotoxic radionuclides with β-, Auger, or α-emissions.

Key Words: monoclonal antibody; CD19; Philadelphia chromosome–positive acute lympoblastic leukemia; severe combined immunodeficient mouse strain

J Nucl Med 2003; 44:1105–1112

The treatment of childhood acute lymphoblastic leukemia (ALL) with chemotherapy has had cure rates of up to 80% (*1*). Adults with ALL, however, have much lower cure rates. In particular, the subset of patients with the Philadelphia chromosome translocation (Ph$^+$) have poor prognosis (*2*,*3*). A suitable mouse model for the study of ALL is the severe combined immunodeficient (SCID) mouse strain. These mice are deficient in functional T- and B-cells with very low levels of circulatory immunoglobulins (*4*). We and others have shown that primary human leukemias engrafted into SCID mice disseminate in a pattern analogous to human disease, with the presence of malignant cells in blood, bone marrow, and infiltration of peripheral organs such as spleen and liver (*5*). In general, the xenograft human leukemia requires the SCID mouse environment and cannot be maintained in vitro. This SCID mouse model has been successfully used to evaluate novel therapies, including interleukin-4 (*5*) and liposomal vincristine (*6*), in an acute leukemia setting.

Clusters of differentiation 19 antigen (CD19) are B-cell–specific molecules expressed on virtually all human cells (except plasma cells) of the B-lymphocyte lineage. CD19 is a critical signal transduction molecule that regulates B-lymphocyte development, activation, and differentiation (*7*). The CD19 molecule is associated with membrane and

Received Nov. 18, 2002; revision accepted Mar. 5, 2003.

For correspondence or reprints contact: Fook-Thean Lee, PhD, Ludwig Institute for Cancer Research, Austin and Repatriation Medical Centre, 145-163 Studley Rd., Heidelberg, Victoria 3084, Australia.

E-mail: ft.lee@ludwig.edu.au

intracellular signaling proteins in the regulation of these cellular processes. Engagement of CD19 with monoclonal antibody (mAb) has been shown to induce apoptosis in B-lineage ALL cells (*8*). In addition, CD19 undergoes antibody-induced end capping or redistribution, followed by internalization and routing to nuclear membrane via the endoplasmic reticulum (*9*).

The anti-CD19 mAb CLB-CD19 (IgG1κ) has been developed and was shown to inhibit B-cell proliferation (*10*). The class-switched variant CLB-CD19 (IgG2a) was evaluated in a small group of patients with non-Hodgkin's lymphoma, with partial and minor responses observed (*11*). Targeting CD19 with mAb holds promise for the treatment of leukemia and lymphoma because the antigen expression is maintained in malignant B-lineage cells (*12*). Another antibody conjugated to the CD19 receptor associated tyrosine kinase inhibitor (Genistein) has also been evaluated in patients with ALL (*13*), with objective clinical responses observed.

We report the targeting of human Ph^+ ALL engrafted in SCID mice using ^{111}In- but not ^{125}I-labeled CLB-CD19 mAb ($IgG1_\kappa$). CLB-CD19 mAb by itself had a delayed suppressive effect on the circulatory levels of ALL cells. To our knowledge, the use of a SCID mouse model developed from primary patient ALL in mAb-targeted therapy has not been reported previously. We also discuss the implications of such results and therapeutic opportunities possible with this approach.

MATERIALS AND METHODS

Antibodies and Cells

The hybridoma for the murine anti-CD19 mAb CLB-CD19 (IgG1κ) was provided by Dr. Gijs van Schijndel (Netherlands Red Cross, Amsterdam, The Netherlands) and was cultured in Iscove's modified Dulbecco's medium containing 10% (v/v) fetal bovine serum (FBS) (CSL Ltd.). The hybridoma for the isotype-matched control murine anti-CD30 mAb, HRS-3, was provided by Prof. Michael Pfreundschuh (University of Saarland, Homburg, Germany) and was cultured in RPMI 1640 medium containing 10% (v/v) FBS and 100 nmol/L methotrexate (Invitrogen). CLB-CD19 and HRS-3 were produced in the Biological Production Facility (Ludwig Institute for Cancer Research, Melbourne, Victoria, Australia). CD19-positive ($CD19^+$) Daudi cells were used as a target for radiolabeled anti-CD19 antibody and were obtained from the American Type Culture Collection. CD30-expressing L540 cells used for isotype-matched control antibody HRS-3 were provided by Prof. M. Pfreundschuh. Daudi and L540 cells were grown in RPMI 1640 medium (Trace Biosciences Pty. Ltd.) with 10% (v/v) FBS.

Radiolabeling and Quality Assurance

All analytic-grade reagents, except when stated, were obtained from Merck Pty. Ltd. The mAb CLB-CD19 was trace labeled with ^{125}I (GeneWorks; NEN) via tyrosine residue(s) using the standard chloramine-T method as described (*14*) and purified on a centrifugal desalting column equilibrated in phosphate-buffered saline (PBS) (*14*). Radioactivity was measured with an Atomlab-100 dose calibrator (Biodex). Radiochemical purity of labeled antibody was analyzed by instant thin-layer chromatography (ITLC-SG; Gelman Sciences Inc.), developed using 10% (w/v) trichloroacetic acid as solvent, and radioactivity was measured with a Cobra II automated γ-counter (Canberra-Packard) (*14*).

The antibody CLB-CD19 was also labeled with ^{111}In (MDS Nordion) via the bifunctional metal ion chelate CHX-A″-diethylenetriaminepentaacetic acid (DTPA) according to methods described previously (*14*). Briefly, CLB-CD19 was conjugated with the chelate at 3-fold molar excess concentration, purified by dialysis, and stored as aliquots at −80°C. For radiolabeling, ^{111}In-acetate was added to 100 μL of chelated CLB-CD19 (5.6 mg/mL) and the pH was maintained at pH 5.5 by addition of 1.0N HCl. After 20 min, the pH was increased by adding 2.0 mol/L sodium acetate and then the reaction was quenched with 1.0 mmol/L ethylenediaminetetraacetic acid (EDTA). The radiolabeled antibody was purified by Sephadex G50 chromatography (Sigma Chemical Co.) using 10 mmol/L phosphate buffer containing 0.15 mol/L NaCl, pH 7.2 (PBS), as solvent. The radiochemical purity of ^{111}In-labeled antibodies was analyzed by ITLC-SG developed using 10 mmol/L EDTA and a 0.9% (w/v) saline/10 mmol/L NaOH mixture. For controls, the mAb HRS-3 was similarly radiolabeled with ^{125}I and ^{111}In.

The immunoreactivities of radiolabeled antibody CLB-CD19 were determined using the assay of Lindmo et al. (*15*). Twenty nanograms of radiolabeled antibodies were added to $0–4.0 \times 10^7$ Daudi cells in 1.0 mL of media. The cells were kept in suspension through slow rotation and incubated at room temperature for 45 min. Cells were harvested by centrifugation after 2 washes with media to remove unbound antibody. Cell pellets were counted for radioactivity together with 3 aliquots of standards using a γ-counter. The percentage of binding of radiolabeled antibodies was calculated by the formula: (cpm cell pellet/mean cpm radioactive standards) × 100. The percentage binding was graphed against Daudi cell concentration, and immunoreactivities were calculated as the *y*-intercept of the inverse plot of both values. For Scatchard assay, increasing amounts of unlabeled CLB-CD19 (0–10 μg) were mixed with 20 ng of radiolabeled antibody before addition of 1.5×10^7 Daudi cells. The extent of radiolabeled antibody binding was determined as described above and plotted as (specific bound)/reactive free versus (specific bound) (*15*). The association constant (K_a) was derived from the slope of the plot, and the number of antibody-binding sites was obtained from the intercept on the *x*-axis.

The serum stability of radioconjugates after radiolabeling was determined by incubation in human serum at 37°C over 6 d. The extent of radioisotope bound to protein and the immunoreactivities were determined by ITLC-SG and the cell-binding assay, respectively, on days 0 and 6 as described above.

Animal Models

Peripheral blood leukemia cells were obtained from a patient diagnosed with Ph^+ common ALL as described (*5*). ALL cells were injected intravenously into sublethally irradiated female SCID mice. Single-cell suspensions of murine spleen, containing >95% human ALL cells, were obtained from engrafted mice and administered intravenously to additional SCID mice. Splenic single-cell suspensions were obtained, cryopreserved in RPMI media containing 5% (v/v) dimethyl sulfoxide, and shipped to the Ludwig Institute, Melbourne, Victoria, Australia. The phenotype of ALL cells was tested for human $CD10^+$ (81%), $CD19^+$ (87.4%), $CD34^+$ (70.5%), and $HLA\text{-}DR^+$ (97.9%) by flow cytometry (Department

of Pathology, Austin and Repatriation Medical Centre, Melbourne, Victoria, Australia). Archived single-cell suspensions were purified via ficoll and injected intravenously into naive 5- to 6-wk-old female SCID mice (Animal Resource Centre, Perth, Western Australia, Australia) housed in autoclaved microisolator cages under positive pressure (Thoren Caging systems Inc.). Single-cell suspensions obtained from the ALL-infiltrated spleens of these animals were washed twice with RPMI media and 2.0×10^7 cells prepared in 0.1 mL PBS, then injected into SCID mice via the tail vein. From 2 wk after injection of cells, aliquots of blood were collected from the tail vein of mice and analyzed for murine and human cells by flow cytometry as described below.

Immunohistochemistry

At 24 d after injection of ALL cells into SCID mice, enlarged spleen and tumor-bearing liver were quickly removed and snap-frozen in isopentane. Sections of 5-μm thickness were cut using a cryomicrotome (Microm HM5000; Zeiz). All immunohistochemical reagents used were from Sigma. Sections were fixed in buffered formalin, and nonspecific binding was treated with protein-blocking agent for 10 min (Immunon). Human CD19 antigen was detected using murine CLB-CD19 mAb (10 μg/mL in 1% bovine serum albumin/PBS) as primary antibody by incubation for 60 min at room temperature. Horseradish peroxidase–conjugated anti-mouse antibody was used to detect bound mAb with 3-amino-9-ethylcarbazole as chromogen and hematoxylin as the counterstain. For controls, the isotype-matched murine HRS-3 mAb was used.

Flow Cytometry Analysis

Aliquots of blood (20 μL) were collected from the tail vein of mice, added to 50 μL of PBS in a heparin-coated tube, and centrifuged (900 rpm, 2 min). The cell pellet was gently suspended in 5 μg/mL phycoerythrin (PE)-conjugated antimurine CD45 (Immunotech) and 5 μg/mL PE-Cy 5-conjugated antihuman CD45 (Southern Biotechnology Associates) and then mixed at 4°C for 30 min protected from light. Cells were centrifuged as before and resuspended in 0.5 mL red blood cell lysis buffer (Optilyse C; Immunotech) and incubated for 15 min at 4°C. An additional 1.0 mL PBS was then added to the lysates; after 15 min at 4°C, cells were collected by centrifugation. Cells were then resuspended in 0.5 mL of 1.0% (v/v) formaldehyde containing PBS. Windows were gated to detect tagged mouse and human cells by flow cytometry (EPICS XL-MCL; Beckman-Coulter) with a minimum number of 2,000 events recorded. The total number of $CD45^+$ white blood cells was determined (murine plus human $CD45^+$ cells) and the percentage of total for each $CD45^+$ population was calculated.

Infiltration of bone marrow by injected leukemia cells was monitored using flow cytometry. Entire femurs from 2 mice were obtained after killing animals at several time points after injection of leukemia cells. Bone marrow was flushed out using a 29-gauge needle and syringe containing 0.5 mL RPMI media. The proportions of cells expressing human and murine CD45 were detected using flow cytometry as described above.

Biodistribution of ^{125}I- and ^{111}In-CHX″-DTPA CLB-CD19

Doses containing a sterile filtered mixture containing ^{125}I-CLB-CD19 (5 μg, 0.19 MBq) and ^{111}In-CHX-A-DTPA CLB-CD19 (5 μg, 0.24 MBq) in 0.1 mL PBS were administered via the tail vein of female SCID mice. Leukemia-engrafted mice were dosed 26 d after injection of ALL cells. At several time points from 0.25 h after injection, groups of 5 mice were killed by inhalation of ethrane and cranial dislocation. Blood, tumors, and various tissues were removed and blotted dry for weighing and radioactive counting, together with standards, in a γ-counter. Windows were set for ^{125}I (15–75 keV) and ^{111}In (140–430 keV) dual-isotope counting with appropriate spill down and up corrections. The results of radiolabeled antibody biodistribution over time were expressed as the percentage injected dose per gram of blood or tissue (%ID/g) and as tumor-to-blood ratios. For controls, ^{125}I- and ^{111}In-labeled HRS-3 were similarly injected into leukemia-engrafted mice and sacrificed at 4 and 24 h after injection Another control group consisted of administering radiolabeled CLB-CD19 in mice without leukemia to demonstrate the biodistribution properties of the radioconjugate of interest.

Gamma-Camera Imaging

To visualize the distribution of radioconjugates in the whole body, mice with and without engrafted leukemia were selected randomly from the groups of animals used for the biodistribution studies. At time points 24, 48, and 72 h after injection of radiolabeled CLB-CD19, animals were anesthetized by intraperitoneal injection of 0.2 mL solution containing 18.7 mg/mL tribromoethanol dissolved in 12.5 μL isopentyl alcohol/mL of water for injection. Images were obtained using a dual-head Biad gamma camera (Trionix) equipped with a medium-energy collimator. ^{111}In images were acquired over 10 min and data were recorded on a SunSparc Station 10 computer (Sun Microsystems Europe Inc.).

Effect of Single Injection of Unconjugated CLB-CD19

A preliminary therapeutic study was conducted in 2 groups of 8 mice engrafted with ALL cells (passage no. 6). On day 26 after injection of tumor cells, groups of 8 mice were treated intravenously either with saline or with 32 μg of unlabeled CLB-CD19 antibody. HRS-3 antibody was not used as a subclass control because this radiolabeled antibody did not localize to the tumor (Results). Blood from mice was collected via the tail at various times after injection of cells and analyzed using flow cytometry for murine and human white cells expressing CD45 as before.

Statistics

The survival of the control and the treatment groups was compared using Kaplan–Meier analysis and statistical differences analyzed using the log rank test (Prism; GraphPad Software Inc.). Mean uptakes of radiolabeled antibodies into tumor and normal tissue were compared by a *t* test.

RESULTS

Antibody Radiolabeling

The CLB-CD19 mAb was radiolabeled to specific activities of 37.5 and 48.8 MBq/mg for ^{125}I and ^{111}In, respectively. The immunoreactivities, as determined by the assay of Lindmo et al. (*15*), were 80% and 79%, respectively. The respective K_a values, as determined using the Scatchard assay, were 6.6×10^8 mol/L^{-1} and 5.6×10^8 mol/L^{-1}, with 37,600 and 46,000 antibody-binding sites per Daudi cell, respectively. The radioconjugates were relatively stable when incubated in human serum for 6 d at 37°C, whereas the immunoreactivities of ^{125}I- and ^{111}In-conjugates decreased to 56.5% and 64.9%, respectively (data not shown).

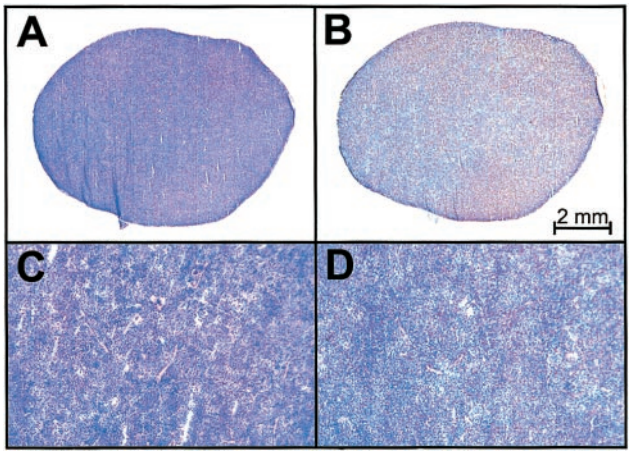

FIGURE 1. Histologic analysis of spleen obtained from SCID mouse engrafted with primary Ph^+ ALL cells. Photomicrographs (×5) of hematoxylin- and eosin-stained splenic section (A) show extensive infiltration of leukemia cells expressing CD19 antigen (B). (C and D) Corresponding sections (×25) demonstrate lack of tissue architecture due to leukemia infiltration. When isotype control antibody was used, no staining was observed (data not shown).

Engraftment of Leukemia Cells

Primary human ALL cells, obtained directly from patients, disseminate in engrafted mice in a pattern that resembles the human disease (*5*). In this study, we limited the analysis of leukemia cells to blood, bone marrow, spleen, and liver for demonstrating disease engraftment, targeting of radioconjugates, and antitumor effect of CLB-CD19 antibody. Leukemia cells were virtually undetectable in blood for up to 3 d after injection of cells but became prominent at later time points (see below). At postmortem on day 26, the enlarged spleen was infiltrated with $CD19^+$ leukemia cells as demonstrated through hematoxylin and antigen staining of tissue sections (Fig. 1). Leukemia cells were distributed throughout the spleen. Similarly, leukemia cells also infiltrated the mouse liver, but to a lesser extent (data not shown). Flow cytometric analysis of bone marrow aspirates indicated that the proportion of human cells reached 73.17% ± 8.87% (mean ± SD) by day 17 after injection of ALL cells (data not shown).

Biodistribution

The biodistribution results for radiolabeled CLB-CD19 and isotype control HRS-3 are presented in Tables 1 (^{125}I) and 2 (^{111}In). Biodistribution studies indicated that both the ^{125}I- and ^{111}In-conjugate of CLB-CD19 were present in low concentrations (1.5–2.5 %ID/g) in the blood even at the earliest time point of 15 min after injection (Tables 1 and 2). Over the 5-d study period, the concentration of radioconjugates in the blood remained low. This suggests that both the ^{125}I- and ^{111}In-conjugates of anti-CD19 were rapidly taken up by leukemia infiltrates lodged in the spleen and, to a lesser extent, the liver. The mean ± SD maximal uptake of ^{111}In-CLB-CD19 in spleen occurred at 24 h after injection (72.78 ± 13.67 %ID/g). In contrast, the ^{125}I-conjugate of CLB-CD19 was initially present in the spleen at comparatively lower levels but, by 24 h after injection, the radioactivity had dropped to very low levels. The mean tumor (spleen)-to-blood ratio for ^{111}In-CLB-CD19 increased from 5.9:1 (0.25 h after injection) to 21.0:1 (24 h after injection). Uptake of radioconjugates in the ALL-infiltrated liver also showed a similar trend (Tables 1 and 2). Minimal uptake (0.1–3.6 %ID/g) was observed in normal tissues at all time points (data not shown).

To demonstrate specific targeting of leukemia cells in spleen, 2 other biodistribution studies were performed. The first study involved injecting ^{125}I- and ^{111}In-conjugated HRS-3 isotype-matched control into disease-bearing mice (Tables 1 and 2). The blood concentrations of control conjugates were normal (20.89–21.59 %ID/g) at 24 h after injection, and the mean spleen-to-blood and liver-to-blood ratios were in the range 0.35:1 to 0.7:1, indicating a lack of specific uptake. The localization ^{125}I- and ^{111}In-controls were similar in these 2 organs, unlike radiolabeled CLB-CD19 mAb. In the second control study, the same dose of ^{125}I- and ^{111}In-conjugated CLB-CD19 was injected into

TABLE 1
Biodistribution of ^{125}I-CLB-CD19 and Control Antibody in ALL-Engrafted SCID Mice

	%ID/g*						
Organ	0.25 h†	4 h†	24 h†	48 h†	72 h†	120 h†	Control‡ 24 h
Blood	2.51 ± 0.18	10.02 ± 4.89	5.48 ± 1.29	2.92 ± 0.38	2.16 ± 0.35	7.24 ± 4.37	20.89 ± 3.07
Liver	15.55 ± 5.55	7.97 ± 1.50	0.32 ± 0.63	0.00 ± 0.00	0.00 ± 0.00	2.64 ± 1.98	10.63 ± 1.16
Spleen	10.32 ± 4.47	11.41 ± 12.79	0.02 ± 0.01	0.00 ± 0.00	0.00 ± 0.00	2.17 ± 1.71	7.48 ± 1.36
Kidney	3.76 ± 1.57	4.61 ± 2.08	1.33 ± 1.09	1.13 ± 0.17	0.24 ± 0.23	2.17 ± 1.22	6.03 ± 0.47
Bone	1.90 ± 1.13	3.35 ± 2.23	1.52 ± 0.53	0.70 ± 0.11	0.23 ± 0.27	1.06 ± 0.62	2.36 ± 0.18
Lung	8.30 ± 1.48	9.35 ± 2.74	2.58 ± 0.78	1.29 ± 0.23	0.91 ± 0.23	2.91 ± 1.39	8.28 ± 0.38
Stomach	3.72 ± 2.18	13.88 ± 11.44	9.81 ± 3.34	3.36 ± 1.43	2.69 ± 0.67	2.82 ± 1.49	3.27 ± 1.61

*Values are expressed as mean ± SD, where $n = 5$ (except at 120 h, where $n = 3$ or 4).
†Time after injection of radioconjugate.
‡Control consists of ^{125}I-HRS-3 at 24 h after injection.

TABLE 2
Biodistribution of ^{111}In-CHX-A″-DTPA CLB-CD19 and Control Antibody in ALL-Engrafted SCID Mice

Organ	%ID/g*						
	0.25 h†	4 h†	24 h†	48 h†	72 h†	120 h†	Control‡ 24 h
Blood	1.51 ± 0.17	7.31 ± 4.03	3.46 ± 1.14	1.58 ± 0.35	1.41 ± 0.48	5.55 ± 3.80	21.59 ± 3.11
Liver	20.46 ± 7.35	21.76 ± 7.41	22.10 ± 11.04	8.80 ± 0.34	12.66 ± 3.73	8.14 ± 1.21	15.32 ± 1.48
Spleen	8.89 ± 3.54	43.69 ± 35.60	72.78 ± 13.67	42.45 ± 11.33	31.91 ± 3.72	7.58 ± 3.49	9.37 ± 1.59
Kidney	3.41 ± 1.26	5.04 ± 2.54	7.97 ± 1.86	7.01 ± 1.66	3.96 ± 0.68	4.40 ± 1.46	7.59 ± 0.58
Bone	1.65 ± 0.96	3.44 ± 2.87	9.41 ± 3.56	6.75 ± 3.18	5.62 ± 4.26	5.37 ± 3.21	2.65 ± 0.22
Lung	8.67 ± 1.05	10.95 ± 3.48	5.44 ± 0.73	3.97 ± 0.65	2.50 ± 0.55	6.45 ± 3.51	12.23 ± 1.26
Stomach	2.48 ± 1.81	2.16 ± 0.91	1.54 ± 0.38	0.90 ± 0.10	0.65 ± 0.08	0.99 ± 0.62	2.36 ± 0.95

*Values are expressed as mean ± SD, where $n = 5$ (except at 120 h, where $n = 3$ or 4).
†Time after injection of radioconjugate.
‡Control consists of ^{111}In-CHX-A″-DTPA HRS-3 at 24 h after injection.

SCID mice without leukemia and analyzed for biodistribution at 2 time points. At 4 h after injection, the biodistribution of ^{111}In-CLB-CD19 was unremarkable, present in high concentrations in blood (37.82 ± 8.59 %ID/g), spleen (10.67 ± 1.39 %ID/g), and liver (15.68 ± 2.69 %ID/g). By 24 h after injection, the concentrations in blood dropped to 18.97 ± 9.11 %ID/g, spleen uptake increased to 13.18 ± 2.42 %ID/g, and liver uptake decreased to 10.88 ± 0.67 %ID/g. These values were comparable with that of ^{111}In-control antibody, indicative of normal blood clearance and tissue distribution. The values for ^{125}I-CLB-CD19 were essentially similar to that for ^{111}In-conjugate at both of these time points (data not shown). Blood values at 120 h were slightly elevated for both ^{125}I- and ^{111}In-constructs, which resulted in some normal organs having higher uptake values than at 72 h. However, in all cases, these values were low (2–3 %ID/g) and were consistent with minor experimental variations. These results suggest that both ^{125}I- and ^{111}In-conjugates of anti-CD19 were stable in vivo without significant uptake in normal spleen and liver.

The uptake of ^{111}In-CLB-CD19 in bone (9.41 ± 3.56 %ID/g at 24 h) in engrafted mice was significantly higher than that for the ^{111}In-HRS-3 control (2.65 ± 0.22 %ID/g; $P = 0.003$). This uptake was likely due to the leukemia-infiltrated marrow within the bone cavity.

Gamma-Camera Imaging

Localization of ^{111}In-CHX-A″-DTPA CLB-CD19 to leukemia-infiltrated spleen was readily detectable by gamma-camera imaging. Scintigraphic images clearly showed the uptake of ^{111}In-conjugate by 24 h (Fig. 2). At 24 h after injection, the mean spleen-to-blood ratio was 21:1 and the mean liver-to-blood ratio was 6.4:1. At 48 h after injection, the mean ratios were 26.9:1 and 5.6:1. In contrast, gamma-camera images of normal mice without leukemia indicated blood pool in the heart and lung areas by 24 h after injection with diminishing activity at 72 h after injection These results were consistent with the biodistribution properties of the radioconjugates in the control mice.

Effects of CLB-CD19 mAb Therapy in ALL-Engrafted SCID Mice

The effect of CLB-CD19 on circulatory ALL cells and ALL-engrafted SCID mice was evaluated by flow cytometry and animal survival. The levels of circulatory ALL cells was monitored by analysis of blood taken from 2 groups of engrafted mice at various time points (Fig. 3). One group of mice ($n = 8$) was treated with 32 μg CD19-CLB on day 26 after injection of cells, and a second group of control animals ($n = 8$) received saline vehicle. Isotype-matched control antibody HRS-3 was not used because this antibody

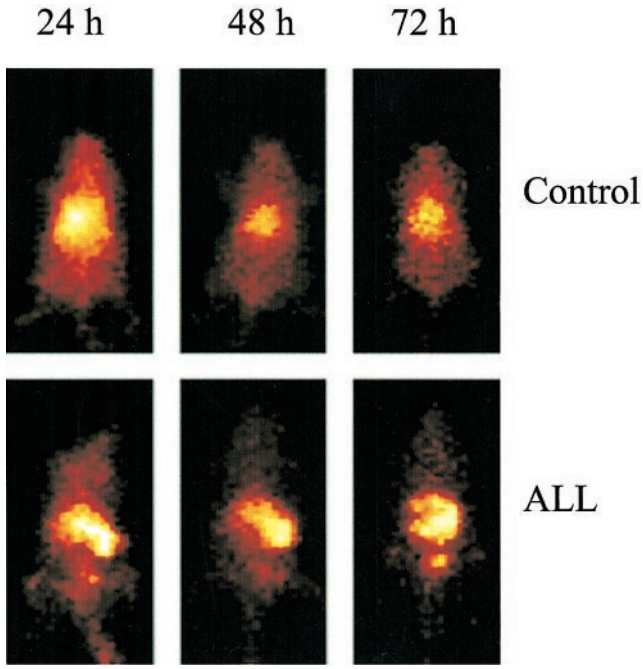

FIGURE 2. Whole-body gamma-camera images at 24, 48, and 72 h after injection. ^{111}In-CHX-A″-DTPA CLB-CD19 for control SCID mice shows activity associated with blood pool (top row) and ALL-engrafted mice with spleen infiltrates (bottom row).

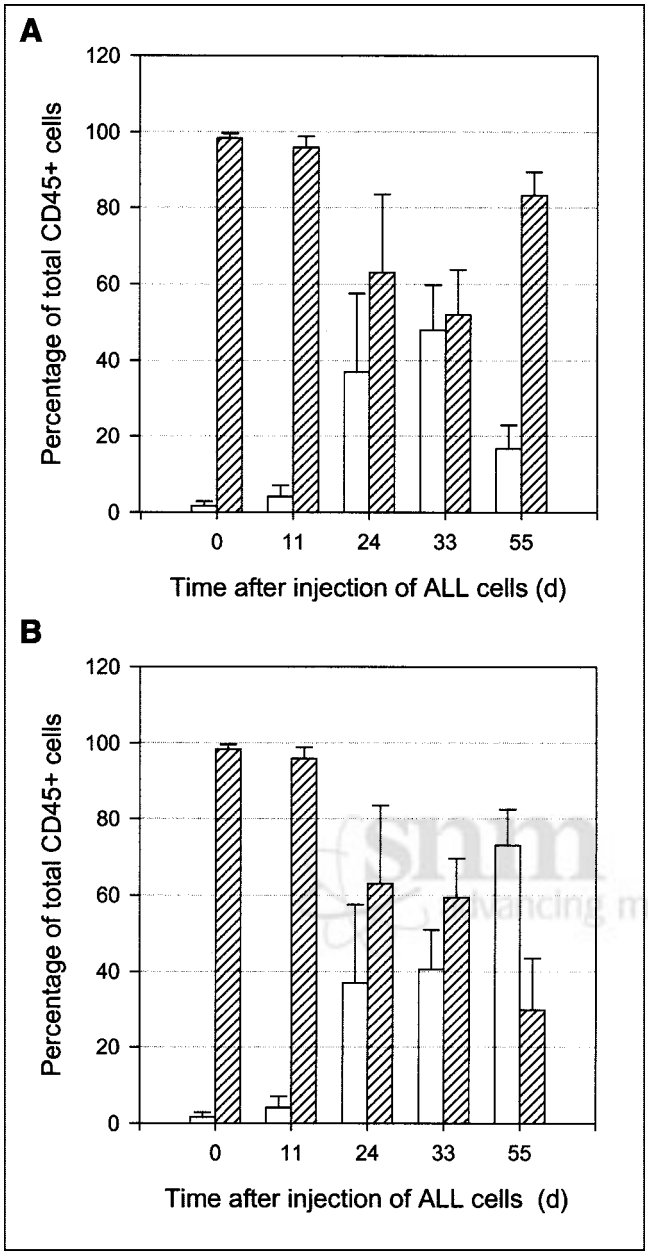

FIGURE 3. Flow cytometric analysis of blood collected at various time points from SCID mice injected intravenously with 20×10^6 Ph^+ ALL cells on day 0. Groups of mice ($n = 8$) were treated intravenously with CLB-CD19 antibody (A) or saline vehicle (B) on day 26. The mean ± SD proportion of human (open bars) and murine (hatched bars) cells expressing human or murine CD45, respectively, was expressed as percentage of total $CD45^+$ white blood cells at each time point.

did not show specific targeting, as demonstrated in the biodistribution studies.

Until day 11 after injection of leukemia cells, levels of ALL cells in the blood were low (Fig. 3). Subsequently, the proportion of ALL cells increased. At day 33, all mice were alive in both groups and the percentage of ALL cells in the blood in the antibody-treated group (mean ± SD, 47.98% ± 11.72%) was comparable to levels in the blood of the vehicle control group (40.64% ± 10.29%; $P = 0.323$). CLB-CD19 treatment was administered on day 26 after injection of ALL cells (Fig. 3). By day 55 after injection of cells (29 d after CLB-CD19 treatment), all mice in the antibody-treated group were alive compared with only 2 alive in the saline group. The proportion of human ALL cells within the antibody-treated group was significantly lower at day 55 (16.73% ± 6.0%) compared with day 33 (47.98% ± 11.72%; $P < 0.001$). The level of ALL cells was also lower at day 55 compared with the saline control group (73.08% ± 9.44%; $P < 0.001$).

The median survival of the control group was 49.5 d compared with 58 d for the CLB-CD19 antibody treatment group. There was a statistical difference in survival between the 2 groups ($P = 0.039$; log rank test.) However, the mice in the antibody-treated group subsequently died over a short period of 3 d (day 56–59).

DISCUSSION

The use of mAbs for the treatment of hematologic malignancies has been successfully demonstrated in patient trials. Both anti-CD20 mAb (rituximab [Rituxan]; IDEC Pharmaceutical Corp.) and ^{90}Y-anti-CD20 (^{90}Y-ibritumomab tiuxetan [Zevalin]; IDEC Pharmaceutical Corp.) have been approved for the treatment of low-grade non-Hodgkin's lymphoma by the Food and Drug Administration (FDA). Anti-CD20 mAb alone induces apoptosis and cell death through immune-mediated mechanisms (*16*). Treatment of patients with low-grade lymphoma with anti-CD20 mAb has been shown to be more effective if the antibody is labeled with a cytotoxic isotope such as ^{131}I or ^{90}Y (*17*). For leukemia, the use of humanized anti-CD33 conjugated to calicheamicin has shown clinical usefulness in a defined patient population with acute myeloid leukemia and has been recently approved by the FDA for this condition (*18*). The CD19 antigen has also emerged as an attractive target for mAb-based therapy because of its expression in a broad range of B-cell malignancies (*7,10–12*)

Radiolabeled antibodies are extremely useful for evaluating biodistribution properties of antibodies. The properties of radiohalogen (e.g., ^{125}I) and radiometals (e.g., ^{111}In) used for radiolabeling antibodies have an effect on the retention of the radioconjugates, depending on the internalization mechanisms of the target antigen on the tumor cell. Upon internalization of the antibody–antigen complex, an internalization pathway involving translocation to lysosomes leads to radiometals rather than radioiodine being preferred for labeling internalized antibodies. Tumor lysosomal trafficking and catabolism of radioconjugates usually results in the retention of radiometals compared with loss of iodotyrosine from tumor cells when conventional radioiodination has been performed (*14*). The purpose of this study was to prepare stable ^{125}I- and ^{111}In-conjugates of CLB-CD19 antibody and compare their biodistribution properties in a novel ALL-engrafted SCID mouse model that has a close

resemblance to human ALL. In addition, the use of the 2 radiolabeled conjugates provided an insight into the intracellular destination of the antibody–antigen complex and kinetics of catabolism of internalized antibody.

Both ^{125}I- and ^{111}In-conjugates of CLB-CD19 were shown to have similar and favorable properties in vitro. The difference in uptake in leukemia deposits in the spleen and liver between ^{125}I and ^{111}In is likely to be attributable to internalization of the antibody–antigen complex and translocation via endosomes. Late-stage endosomes rapidly fuse with lysosomes where enzymatic degradation occurs with retention of ^{111}In-catabolites but loss of ^{125}I-catabolites. There have been several other studies in CD19 tumor systems supporting this hypothesis. Three ^{125}I-anti-CD19 mAbs (HD37, B4, SJ25-C1) were shown to be internalized by Ramos Burkitt's lymphoma cells (*19*). The intracellular degradation rates in this study varied from 11% to 41% over 24 h. The CD19 antigen undergoes antibody-induced modulation and has been shown using immunogold electron microscopy to be internalized into the NALM-6 cell line and transported to lysosomes (*20*). It has also been shown, using confocal microscopy, immunofluorescence, and immune electron microscopy in CD77$^+$ Daudi cells, that anti-CD19 mAb B4 induces CD19 cell-surface redistribution, internalization, and routing to the nuclear envelope and induction of apoptosis (*9*).

We have shown that the blood clearance of radiolabeled CLB-CD19 was rapid. This rapid clearance was most likely due to radioconjugate uptake by leukemia infiltrates in spleen, liver, and marrow. The implications of this in treating ALL with β-radiolabeled anti-CD19 mAb is that myelotoxicity is likely to be pronounced as the leukemia cells are intimately mingled with blood-producing cells. Short-range α-emitters (high linear energy transfer values) and Auger electron emitters (e.g., ^{111}In and ^{67}Ga at high doses) may be more effective for inducing radiation damage to DNA if delivered within malignant cells (*21–24*), reducing hematologic toxicity when targeting circulating and bone marrow infiltrates. The more commonly available metallic α-emitter ^{213}Bi has a half-life ($t_{1/2}$) of 45.6 min. This isotope is readily conjugated to antibodies and the short $t_{1/2}$ is compensated for by both the rapid uptake of radioconjugates by leukemia cells and the requirement for only a few α-particles to produce DNA damage (*21*). For less readily accessible disease, medium-energy β-emitters such as ^{177}Lu ($t_{1/2}$ = 6.7 d; $E_{\beta max}$ = 0.50), when accumulated within malignant cells, may also irradiate adjacent cells through the cross-fire effect.

A single injection of 32 μg of unlabeled CLB-CD19 caused a significant lowering of circulatory leukemia cell concentrations. This effect was delayed, taking 1–3 wk to manifest (Fig. 3). Importantly, the lowered ALL cell concentration was also associated with prolonged survival of ALL-engrafted mice with 8 of 8 treated versus 2 of 8 control animals alive at day 55 after injection of cells. There may be several mechanisms for this inhibitory effect. One possibility is the antibody-dependent cellular cytotoxicity (ADCC) effect of the antibody acting through natural killer (NK) cells, even though the levels of NK cells are low in SCID mice. The CLB-CD19 is an IgG1 and we have observed, using the classical ^{51}Cr-release assay, that this antibody has very low or negligible complement-dependant cytotoxicity and ADCC activities (data not shown). Therefore, the therapeutic effect due to these immune effector functions is unlikely to completely explain our observations of prolonged survival. Another possible explanation is inhibition of leukemia cells via apoptosis after engagement of antigen by CLB-CD19 antibody (*12*).

In the study of Hekman et al. (*11*), 2 lymphoma patients had elevated white blood cell counts of 96.2 and 138 × 10^9/L (>90% lymphoma cells by phenotype). An initial dose of 15 mg CLB-CD19 (IgG2a) antibody reduced the concentration of peripheral lymphocytes by 85% within 2 d, but higher doses (30, 60, 120 mg) on subsequent days had progressively smaller effects. By 12 d after antibody dosing, the white blood cell count reached levels similar to that of the pretreatment stage. In this study, cytoreduction, if any, during the first 2 d after injection of antibody was not specifically measured. However, there was significant cytoreduction observed at 31 d after injection in this study (Fig. 3).

Our novel ALL SCID mouse model does not have normal human peripheral blood B-lymphoctyes to act as an antigenic sink. Despite this limitation, the model is useful for evaluating therapeutic approaches, such as dosing regimens with native antibody, antigen modulation, effect of predosing on biodistribution of radiolabeled antibodies, and the effect of radioconjugate by itself and in combination with chemotherapy or other therapies. Because CD19 is widely expressed in B-cell malignancies (*12*), anti-CD19–based therapy has potentially broad application to both B-cell leukemia and lymphoma.

CONCLUSION

We have demonstrated in a novel ALL-engrafted SCID mouse model specific targeting and rapid internalization of radiometals when conjugated to an anti-CD19 antibody (but not radiohalogen) to leukemia infiltrates in spleen, liver, and bone marrow. The antigen dose of anti-CD19 antibody significantly prolonged the survival of ALL-engrafted SCID mice. Further therapeutic studies based on anti-CD19 mAbs in our novel model of ALL are warranted. Anti-CD19 mAbs also have potentially wider applications to other B-cell hematologic malignancies that are refractory to currently available treatment. For repeated use, a reengineered (e.g., chimeric or humanized form) form of CD19 antibody will be required to minimize or eliminate human immune responses to injected antibody.

ACKNOWLEDGMENTS

The authors thank Sam Johnson for technical assistance during this study and Prof. Rene van Lier from the Laboratory for Experimental Immunology, Academic Medical Center, The Netherlands, for facilitating the study. This work was supported in part by the Austin Hospital Medical Research Foundation.

REFERENCES

1. Wheeler KA, Richards SM, Bailey CC, et al. Bone marrow transplantation versus chemotherapy in the treatment of very high-risk childhood acute lymphoblastic leukemia in first remission: results from Medical Research Council UKALL X and XI. *Blood.* 2000;96:2412–2418.
2. Berman E. Recent advances in the treatment of acute leukemia: 1999. *Curr Opin Hematol.* 2000;7:205–211.
3. Schenk TM, Keyhani A, Bottcher S, et al. Multilineage involvement of Philadelphia chromosome positive acute lymphoblastic leukemia. *Leukemia.* 1998;12: 666–674.
4. Leblond V, Autran B, Cesbron JY. The SCID mouse mutant: definition and potential use as a model for immune and hematological disorders. *Hematol Cell Ther.* 1997;39:213–221.
5. Mitchell PL, Clutterbuck RD, Powles RL, et al. Interleukin-4 enhances the survival of severe combined immunodeficient mice engrafted with human B-cell precursor leukemia. *Blood.* 1996;87:4797–4803.
6. Millar JL, Millar BC, Powles RL, et al. Liposomal vincristine for the treatment of human acute lymphoblastic leukaemia in severe combined immunodeficient (SCID) mice. *Br J Haematol.* 1998;102:718–721.
7. Fujimoto M, Poe JC, Hasegawa M, Tedder TF. CD19 regulates intrinsic B lymphocyte signal transduction and activation through a novel mechanism of processive amplification. *Immunol Res.* 2000;22:281–298.
8. Waddick KG, Chae HP, Tuel-Ahlgren L, et al. Engagement of the CD19 receptor on human B-lineage leukemia cells activates LCK tyrosine kinase and facilitates radiation-induced apoptosis. *Radiat Res.* 1993;136:313–319.
9. Khine AA, Firtel M, Lingwood CA. CD77-dependent retrograde transport of CD19 to the nuclear membrane: functional relationship between CD77 and CD19 during germinal center B-cell apoptosis. *J Cell Physiol.* 1998;176:281–292.
10. de Rie MA, Schumacher TN, van Schijndel GM, van Lier RA, Miedema F. Regulatory role of CD19 molecules in B-cell activation and differentiation. *Cell Immunol.* 1989;118:368–381.
11. Hekman A, Honselaar A, Vuist WM, et al. Initial experience with treatment of human B cell lymphoma with anti-CD19 monoclonal antibody. *Cancer Immunol Immunother.* 1991;32:364–372.
12. Scheuermann RH, Racila E. CD19 antigen in leukemia and lymphoma diagnosis and immunotherapy. *Leuk Lymphoma.* 1995;18:385–397.
13. Uckun FM, Messinger Y, Chen CL, et al. Treatment of therapy-refractory B-lineage acute lymphoblastic leukemia with an apoptosis-inducing CD19-directed tyrosine kinase inhibitor. *Clin Cancer Res.* 1999;5:3906–3913.
14. Lee FT, Rigopoulos A, Hall C, et al. Specific localization, gamma camera imaging, and intracellular trafficking of radiolabelled chimeric anti-G(D3) ganglioside monoclonal antibody KM871 in SK-MEL-28 melanoma xenografts. *Cancer Res.* 2001;61:4474–4482.
15. Lindmo T, Boven E, Cuttitta F, Fedorko J, Bunn PA Jr. Determination of the immunoreactive fraction of radiolabeled monoclonal antibodies by linear extrapolation to binding at infinite antigen excess. *J Immunol Methods.* 1984;72:77–89.
16. DeNardo GL, O'Donnell RT, Oldham RK, DeNardo SJ. A revolution in the treatment of non-Hodgkin's lymphoma. *Cancer Biother Radiopharm.* 1998;13: 213–223.
17. Witzig TE, Gordon LI, Cabanillas F, et al. Randomized controlled trial of yttrium-90-labeled ibritumomab tiuxetan radioimmunotherapy versus rituximab immunotherapy for patients with relapsed or refractory low-grade, follicular, or transformed B-cell non-Hodgkin's lymphoma. *J Clin Oncol.* 2002;20:2453–2463.
18. Bross PF, Beitz J, Chen G, et al. Approval summary: gemtuzumab ozogamicin in relapsed acute myeloid leukemia. *Clin Cancer Res.* 2001;7:1490–1496.
19. Press OW, Howell-Clark J, Anderson S, Bernstein I. Retention of B-cell-specific monoclonal antibodies by human lymphoma cells. *Blood.* 1994;83:1390–1397.
20. Pulczynski S. Antibody-induced modulation and intracellular transport of CD10 and CD19 antigens in human malignant B cells. *Leuk Lymphoma.* 1994;15:243–252.
21. Volkert WA, Goeckeler WF, Ehrhardt GJ, Ketring AR. Therapeutic radionuclides: production and decay property considerations. *J Nucl Med.* 1991;32:174–185.
22. Yao Z, Garmestani K, Wong KJ, et al. Comparative cellular catabolism and retention of astatine-, bismuth-, and lead-radiolabeled internalizing monoclonal antibody. *J Nucl Med.* 2001;42:1538–1544.
23. Behr TM, Behe M, Lohr M, et al. Therapeutic advantages of Auger electron- over beta-emitting radiometals or radioiodine when conjugated to internalizing antibodies. *Eur J Nucl Med.* 2000;27:753–765.
24. Govindan SV, Goldenberg DM, Elsamra SE, et al. Radionuclides linked to a CD74 antibody as therapeutic agents for B-cell lymphoma: comparison of Auger electron emitters with β-particle emitters. *J Nucl Med.* 2000;41:2089–2097.